THE JOURNAL OF PHYSICAL CHEMISTRY B LETTERS

2006, *110,* 14028−14031
Published on Web 07/01/2006

Manipulating the Optical Properties of Pyramidal Nanoparticle Arrays

Joel Henzie, Kevin L. Shuford, Eun-Soo Kwak, George C. Schatz, and Teri W. Odom*

Department of Chemistry, Northwestern University, 2145 Sheridan Road, Evanston, Illinois 60208

Received: May 25, 2006; In Final Form: June 16, 2006

This paper reports the orientation-dependent optical properties of two-dimensional arrays of anisotropic metallic nanoparticles. These studies were made possible by our simple procedure to encapsulate and manipulate aligned particles having complex three-dimensional (3D) shapes inside a uniform dielectric environment. Using dark field or scattering spectroscopy, we investigated the plasmon resonances of 250-nm Au pyramidal shells embedded in a poly(dimethylsiloxane) (PDMS) matrix. Interestingly, we discovered that the scattering spectra of these particle arrays depended sensitively on the direction and polarization of the incident white light relative to the orientation of the pyramidal shells. Theoretical calculations using the discrete dipole approximation support the experimentally observed dependence on particle orientation with respect to incident field. This work presents an approach to manipulate−by hand−ordered arrays of particles over cm^2 areas and provides new insight into the relationship between the shape of well-defined, 3D particles and their supported plasmon resonance modes.

The optical properties of metallic nanoparticles are interesting because of their fundamental science and potential for emerging applications. For example, their broad optical tunability from ultraviolet to near-infrared wavelengths can be exploited in nanoscale photonics,[1] chemical and biological sensing,[2] and high-efficiency photovoltaic devices.[3] Electromagnetic radiation can interact with metallic nanoparticles through the resonant excitation of their free electrons. These collective electron density oscillations, confined to a finite volume, are known as localized surface plasmons (LSPs) and are sensitive to the size,[4] shape,[5] and dielectric environment[6] of the nanoparticle.

Both solution-based syntheses and fabrication techniques have been used to generate metallic particles. Most research efforts have focused on the chemical synthesis of nanoparticles because the preparative techniques are relatively straightforward; the size and shape of nanoparticles can be tailored by controlling conditions such as reaction temperature, surfactants, and concentrations of precursors.[5,7] Spherical particles with sizes less than 50 nm support single LSP resonances that are dipolar in character. Accordingly, their optical properties can be explained reasonably well by the lowest order term in Mie theory.[8] In contrast, larger metallic particles (diameters > 100 nm) with anisotropic shapes can exhibit multiple LSP resonances[9,10] that correspond to higher order modes.[11] Disordered assemblies of 100-nm Ag particles embedded in PDMS films showed a dipole resonance as well as a quadrupole resonance as the film was stretched in 2D,[12] and Au rod-shaped particles electrically aligned in aqueous solutions exhibited mostly transverse or longitudinal modes depending on polarization.[13] Because the shape of large metallic particles is often difficult to control by synthetic methods, fabrication techniques have been pursued as an alternative approach. Electron beam lithography can generate particles with arbitrary sizes and shapes in 2D.[14,15] We have recently demonstrated a template-based approach to fabricate 3D metallic pyramidal shells with circular bases, smooth facets, and sharp tips ($r < 2$ nm).[16]

Investigations of submicron particles have only recently been enabled by improved chemical methods to synthesize high-quality crystals and fabrication techniques to generate particles with uniform size and shape. Although multipolar LSP resonances have been seen in the extinction spectra of submicron particles,[9,10] the random dispersion of the particles in solution ensured that all resonant plasmon modes were measured simultaneously, and some peaks were obscured because of polarization averaging. Multipolar excitations can, however, depend on the direction of the wavevector and polarization vector;[17] thus, certain excitation angles can make selected resonances more pronounced.[18] Strategies that can both isolate particles and control their orientation are essential to correlate the orientation of the particles with specific plasmon modes directly. Drop-coating or spin-casting dilute colloidal solutions onto glass slides has resulted in isolated particles although their orientation on the substrate was not well-defined,[19,20] and asymmetric particles were generated by electroless deposition but were closely spaced and still attached to the supporting Au film.[21] Electron beam lithography can create isolated particles with controlled orientation, although the shapes are limited to 2D planar structures.

Here we describe a procedure to generate ordered arrays of well-separated metallic pyramids embedded in a uniform dielectric environment. These 3D nanoparticles are aligned within a single plane and are an ideal system for investigating and identifying multipolar resonances in well-defined structures. We can also interpret and compare their plasmon resonance spectra with computational electrodynamics calculations based on the discrete dipole approximation (DDA).

* Corresponding author. E-mail: todom@northwestern.edu.

10.1021/jp063226i CCC: $33.50

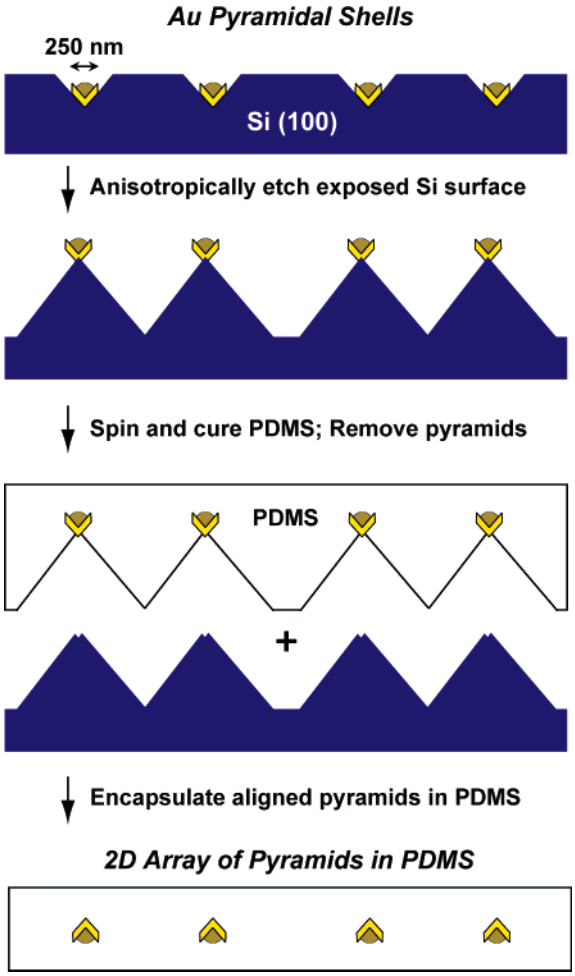

Figure 1. Scheme depicting the transfer and encapsulation of Au pyramids in a PDMS film.

Figure 1 outlines a procedure for transferring Au pyramids situated within the etched pits of a Si(100) mold into a transparent PDMS film. First, the Si substrate containing the Au pyramids (Figure 2A) was subjected to an anisotropic Si etch solution. The pyramids acted as etch masks and protected the underlying silicon; the exposed Si(100) surface was etched quickly, leaving the Au pyramids supported on Si pedestals (Figure 2B). To improve the adhesion between the pyramids and PDMS matrix, the Si substrate was first passivated with tridecafluoro-1,1,2,2-tetrahydrooctyl-1-trichlorosilane (Gelest, Inc.), and the Au pyramids were functionalized with (3-mercaptopropyl) trimethoxysilane (Aldrich).[22] The sample was then pressed against a thin (10 μm) layer of unpolymerized *h*-PDMS[23] and cured. The *h*-PDMS film (with the Au pyramids now partially embedded) was pulled off the substrate with tweezers, and the pyramidal tips protruded partially from the PDMS mold (Figure 2C, inset). We checked that the pyramids were transferred into PDMS by characterizing the etched Si substrate (Figure 2D). To encapsulate the Au pyramids fully, we exposed the array of pyramidal tips to mercaptosilane and then spin-coated a thin (10 μm) layer of *h*-PDMS on top. Figure 2e is a photograph of a large-area PDMS film encapsulating 1-cm^2 array of 250-nm Au pyramids. Additional details of the fabrication process as well as 3D renderings of the pyramids are contained in the Supporting Information.

Dark field (DF) microscopy and spectroscopy were used to characterize the optical properties of the pyramidal particles. Excitation of the arrays was achieved by passing unpolarized or polarized white light through a dark-field condenser (NA = 0.95). The scattered light from the pyramid array was collected using a 20× objective and then analyzed using a spectrometer coupled to a CCD camera. We first characterized a planar array of pyramids whose tips pointed toward the incident light and whose base planes were oriented perpendicular to the optical axis of the microscope (orientation I) (Figure 3A). Figure 3B depicts a DF microscopic image of an array of red spots that correspond to an array of Au pyramidal particles. Note that because 95% of the pyramids in the sample are identical as a result of our top-down lithographic procedure,[16] the spot sizes of the scattered light are uniform, and the color (red) of every spot is the same. The scattered spectrum obtained with unpolarized white light exhibited a strong peak at red wavelengths (~650 nm) and another that appeared to extend into the near-infrared region (Figure 3C). The optical response of this array did not change, however, when the incident light was polarized because the pyramidal particles in this orientation were sym-

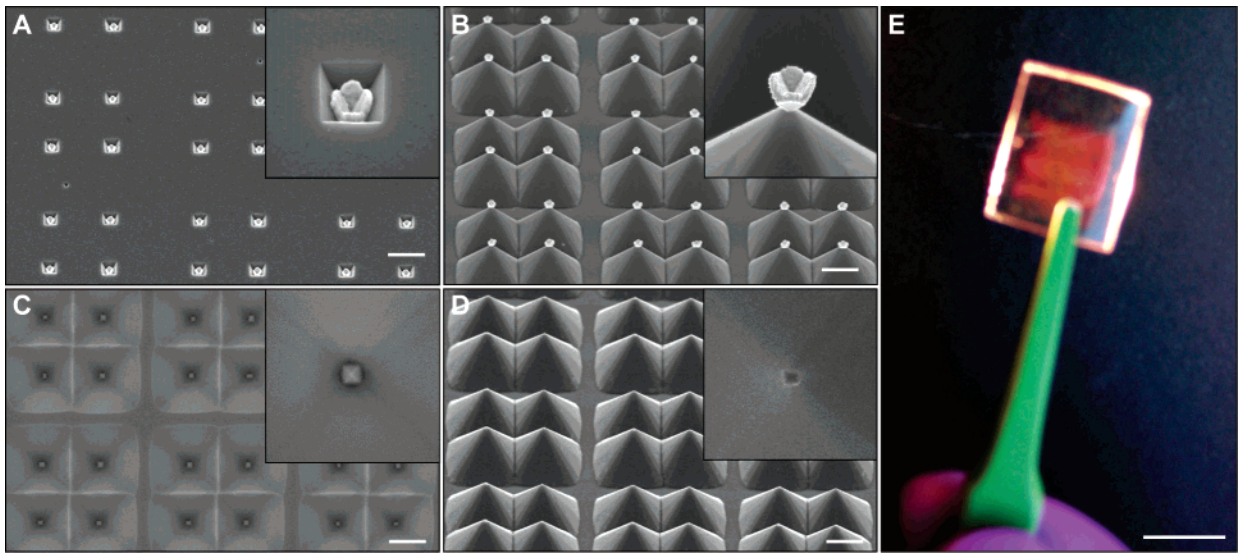

Figure 2. Scanning electron microscope (SEM) images of the key manipulation steps. (A) 250-nm diameter Au pyramids situated in the centers of etched Si pits spaced by ~2 μm. (B) Etched Si(100) pedestals supporting the Au pyramids. (C) Au pyramids transferred and partially embedded within the PDMS film. (D) Etched Si(100) pedestals after removal of the pyramids. The dimensions of all insets are 1 μm × 1 μm, and scale bars are 1 μm. (E) Photograph of a 1-cm^2 pyramid array encapsulated in a thin PDMS film. Scale bar is 1 cm.

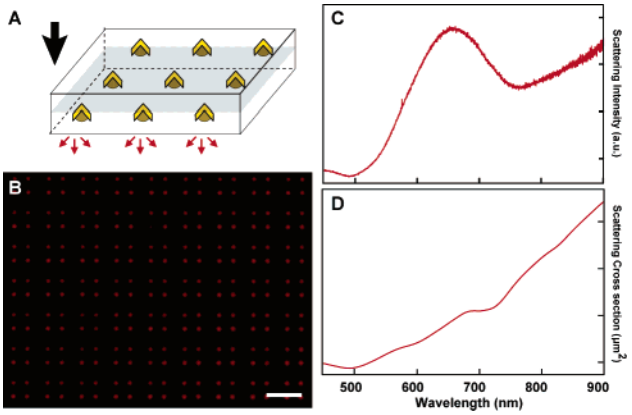

Figure 3. Optical characterization of Au pyramids in an array whose plane is *perpendicular* to the optical axis of the microscope (orientation I). (A) Illustration depicting the geometry of the particle array, the black arrow indicates the direction of the white light source while the gray area denotes the plane of the particle array. (B) Dark field (DF) microscope image of encapsulated Au pyramids with tips pointing directly at the white light source. Scale bar is 4 μm. (C) DF spectrum of the array of Au pyramids. (D) Calculated scattering cross section of a Au pyramidal shell structure in this orientation with the polarization parallel to the base.

metric with respect to the optical axis. Also, the scattering spectrum from the same array with tips pointing *away* from the light source (the PDMS film was flipped over) was identical to the spectra in Figure 3C.

To interpret these spectra, we have performed DDA calculations for a pyramid structure that mimics those fabricated in the experiments. The details are described in the Supporting Information, along with a test of this model that compares results from 100-nm diameter Au pyramids, which support only a dipole resonance. Our DDA calculations here are only for a single pyramid since the separation between the 250-nm Au pyramids is sufficiently large ($\sim$2 μm) that the electromagnetic interactions between them are expected to be weak. Note also that these calculations determine the Rayleigh scattering integral cross section. This cross section is not the same as the angle-resolved cross section measured in the DF spectra, but the same resonance structure should be present.

Figure 3D shows that the calculated theoretical spectrum of a single Au pyramidal shell exhibits a weak peak at 680 nm superimposed on a background that increases at longer wavelengths. An analysis of the induced polarizations from the calculations indicates that the peak at 680 nm is from a quadrupole resonance—localized in the base plane of the pyramid—and that the background increases at longer wavelengths due to the tail of a dipolar excitation that peaks in the near-infrared. Figures 3C and 3D show that experiment and theory are in qualitative agreement, with the main difference being the intensity of the quadrupole resonance. This difference in intensity could result from several factors, including the difference between the calculated integral and angle-resolved cross sections noted above or the sensitivity of the calculations to subtle structural features of the pyramids.

To investigate whether the optical properties of the pyramidal shells depended on their orientation, we exploited the flexible nature of PDMS and sliced the *h*-PDMS film containing the Au pyramids into thin (500 μm) sections. One of these cross-sections was placed on a glass substrate such that the planar array of pyramids as well as the pyramid base planes were *parallel* to the optical axis of the microscope, and the tips were pointed perpendicular to this axis (orientation II) (Figure 4A, inset). Since the orientation of the particles is now *not* symmetric

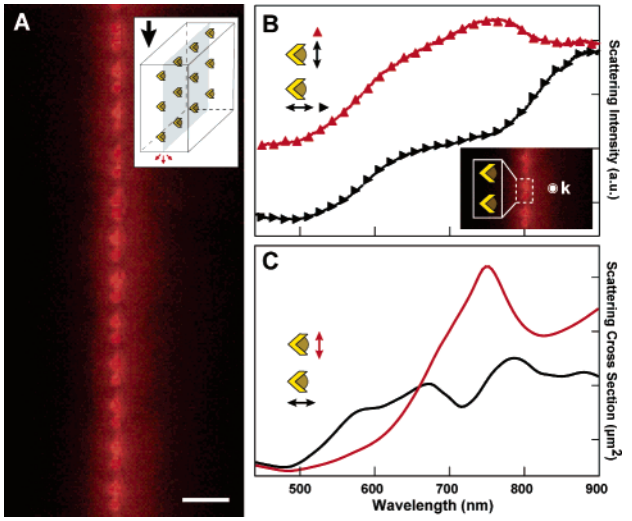

Figure 4. Optical characterization of Au pyramids in an array whose plane is now *parallel* to the optical axis of the microscope (orientation II). (A) DF microscope image of Au pyramids oriented on their sides and whose tips point perpendicular to the white light source. The black arrow in the inset image indicates the direction of the optical axis, and gray area denotes the plane of the particle array. Scale bar is 4 μm. (B) DF spectra of the Au pyramids in (A) illuminated with white light that is polarized parallel to the pyramid base (upward-pointing triangle) and polarized perpendicular to the pyramid base (left-pointing triangle). The inset shows how the pyramids in the array are oriented in (A), and **k** denotes the propagation wavevector, which is parallel to and down the array plane. Both spectra are plotted on the same scale. (C) Calculated scattering cross section of a single Au pyramidal shell in this orientation for two perpendicular polarizations.

with respect to the incident light, we can study the effects of polarization on the scattering spectra. Figure 4A shows a DF image of a thin cross-section of an array with only the bottom layer of pyramids in the depth of focus (hence the scattered light is collected only from a single layer of pyramids). Excitation by unpolarized white light (not shown) produced only broad features in the DF spectra, unlike in orientation I, where unpolarized as well as polarized light produced a defined quadrupole peak. Figure 4B shows the resulting spectra for the cases where the polarization vector is parallel (upward-pointing triangle) and perpendicular (left-pointing triangle) to the base: all polarization directions were defined relative to the base plane. Rotating from parallel to perpendicular polarization produced a color change in the scattered light from deep-red to light-red, respectively, corresponding to the appearance of a resonance peak around 750 nm for the parallel case, and 880 nm for the perpendicular case. When the polarization vector was 45°, the spectra were roughly the average of that from parallel and perpendicular polarization directions and were also similar to the spectra produced from unpolarized white light (see Supporting Information). The calculated spectrum shows a strong resonance at 750 nm for parallel polarization (Figure 4C), in good agreement with the experiment. A polarization vector analysis indicates that this peak is the *same* quadrupole mode localized in the base plane as the one observed for orientation I. The calculated spectrum for the perpendicular polarization indicates the presence of several resonances with an overall envelope that is qualitatively similar to the measured result, except that the intensity of the peak at approximately 880 nm is too weak. Similar to the comparison of results for pyramids in orientation I, the resonance poles of the theoretical calculation match experiment well, but there are some differences in overall peak intensity.

It is interesting that the spectrum for polarization parallel to the base in Figure 4B is red-shifted from the spectrum in Figure 3C, even though they appear at first glance to be optically equivalent. In both cases the polarization vector is parallel to the base, but the wavevectors relative to the base plane are different. In Figure 4B the wavevector is parallel, but in Figure 3C the wavevector is perpendicular. This wavevector dependence typically arises primarily when particles are large compared to the wavelength of light, because the electric field shows significant oscillations along the propagation direction. For example, when the wavevector is perpendicular to the base, the pyramids are relatively "thin," and the excitation field is in-phase at the base of the particle; however, when the wavevector is parallel to the base, the pyramids are relatively "thick," and the excitation field is no longer completely in-phase. These differences can lead to excitation of different superpositions of multipoles, which has the net effect of shifting the nominal wavelength of the dominant multipole, which, for the 250-nm Au pyramids, is the quadrupole mode. In particular, the wavevector parallel to the pyramid base should result in a stronger admixture of *dipolar* excitation, leading to a peak that is red-shifted (Figure 4B) compared to the wavevector perpendicular to the base (Figure 3C). This present experiment and theory comparison is probably the clearest example where this effect has been observed.

In summary, we have demonstrated that arrays of aligned, pyramidal nanoparticles exhibit orientation-dependent optical properties, which were found to be sensitive to both the propagation wavevector and polarization direction. Most importantly, we have begun to correlate the orientation and anisotropic shape of 250-nm particles with specific multipolar plasmon resonances. Such an understanding of these unusual properties of relatively large plasmonic particles, especially those with sharp tips and edges, can be used to enhance the capabilities of plasmon-based applications.

Acknowledgment. This work was supported by the MRSEC program of the National Science Foundation (DMR-0076097) at the Materials Research Center of Northwestern University (NU) and by the URETI program of NASA (under Grant No. NCC 2-1363) subcontracted through Purdue University (under Agreement No. 521) at the MRI of NU. This work made use of the NU*ANCE* Center facilities, which are supported by NSF-MRSEC, NSF-NSEC, and the Keck Foundation. T.W.O. is a DuPont Young Investigator, an Alfred P. Sloan Research Fellow, a Cottrell Scholar of Research Corporation, and a David and Lucile Packard Fellow. G.C.S. and K.L.S. acknowledge DOE grant DEFG02-02-ER15487 for support of this research.

Supporting Information Available: Detailed description of the pyramid fabrication technique, encapsulation of pyramid arrays in PDMS, optical characterization, numerical calculations, and a comparison of experimental and numerical results from 100-nm diameter Au pyramids. This material is available free of charge via the Internet at http://pubs.acs.org.

References and Notes

(1) Oldenburg, S. J.; Hale, G. D.; Jackson, J. B.; Halas, N. J. *Appl. Phys. Lett.* **1999**, *75*, 1063.
(2) Haes, A. J.; Haynes, C. L.; McFarland, A. D.; Schatz, G. C.; van Duyne, R. P.; Zou, S. *MRS Bull.* **2005**, *30*, 368.
(3) Yakimov, A.; Forrest, S. R. *Appl. Phys. Lett.* **2002**, *80*, 1667.
(4) Daniel, M.-C.; Astruc, D. *Chem. Rev.* **2004**, *104*, 293.
(5) Xia, Y.; Halas, N. J. *MRS Bull.* **2005**, *30*, 338.
(6) Jensen, T.; Duval, M.; Kelly, K.; Lazarides, A.; Schatz, G.; Van Duyne, R. *J. Phys. Chem. B* **1999**, *103*, 9846.
(7) Murphy, C. J.; Sau, T. K.; Gole, A. M.; Orendorff, C. J.; Gao, J.; Gou, L.; Hunyadi, S. E.; Li, T. *J. Phys. Chem. B* **2005**, *109*, 13857.
(8) Bohren, C. F.; Huffman, D. R. *Absorption and Scattering of Light by Small Particles*; Wiley: New York, 1998; p 82.
(9) Kumbhar, A. S.; Kinnan, M. K.; Chumanov, G. *J. Am. Chem. Soc.* **2005**, *127*, 12444.
(10) Millstone, J. E.; Park, S.; Shuford, K. L.; Qin, L.; Schatz, G. C.; Mirkin, C. A. *J. Am. Chem. Soc.* **2005**, *127*, 5312.
(11) Shuford, K. L.; Ratner, M. A.; Schatz, G. C. *J. Chem. Phys.* **2005**, *123*, 114713.
(12) Malynych, S.; Chumanov, G. *J. Am. Chem. Soc.* **2003**, *125*, 2896.
(13) van der Zande, B. M. I.; Koper, G. J. M.; Lekkerkerker, H. N. W. *J. Phys. Chem. B* **1999**, *103*.
(14) Canfield, B. K.; Kujala, S.; Kauranen, M.; Jefimovs, K.; Vallius, T.; Turunen, J. *Appl. Phys. Lett.* **2005**, *86*, 183109.
(15) Hicks, E. M.; Zou, S.; Schatz, G. C.; Spears, K. G.; Van Duyne, R. P.; Gunnarson, L.; Rindzevicius, T.; Kasemo, B.; Kall, M. *Nano Lett.* **2005**, *5*, 1065.
(16) Henzie, J.; Kwak, E.-S.; Odom, T. W. *Nano Lett.* **2005**, *5*, 1199.
(17) Kelly, K. L.; Coronado, E.; Zhao, L. L.; Schatz, G. C. *J. Phys. Chem. B* **2003**, *107*, 668.
(18) Krenn, J. R.; Schider, G.; Rechberger, W.; Lamprecht, B.; Leitner, A.; Aussenegg, F. R.; Weeber, J. C. *Appl. Phys. Lett.* **2000**, *77*, 3379.
(19) Mock, J. J.; Barbic, M.; Smith, D. R.; Schultz, D. A.; Schultz, S. J. *J. Chem. Phys.* **2002**, *116*, 6755.
(20) Nehl, C. L.; Grady, N. K.; Goodrich, G. P.; Tam, F.; Halas, N. J.; Hafner, J. H. *Nano Lett.* **2004**, *4*, 2355.
(21) Charnay, C.; Lee, A.; Man, S. Q.; Moran, C. E.; Radloff, C.; Kelley Bradley, R.; Halas, N. J. *J. Phys. Chem. B* **2003**, *107*, 7327.
(22) Childs, W. R.; Nuzzo, R. G. *Langmuir* **2005**, *21*, 195.
(23) Odom, T. W.; Love, J. C.; Wolfe, D. B.; Paul, K. E.; Whitesides, G. M. *Langmuir* **2002**, *18*, 5314.